Comment on the Analysis of Microwave Rotational Zeeman Effect Spectra of Symmetric Top Molecules

L. Engelbrecht * and D. H. Sutter

Abteilung Chemische Physik im Institut für Physikalische Chemie, Universität Kiel

(Z. Naturforsch. **30 a**, 1265—1270 [1975]; received July 7, 1975)

It is pointed out that the translational Lorentz effect which has been neglected in all previous analysis of rotational Zeeman spectra has considerable effects on the overall appearance of the Zeeman multiplets if the rotational transitions show first order Stark effect. This situation occurs for symmetric tops and for E-species transitions of molecules with low barrier internal rotations. Inclusion of the translational Lorentz effect leads to corrections to the published $g_{||}$-values of symmetric tops which are far outside the quoted experimental uncertainties. As an example numerical results are given for CH_3F and CH_3CCH.

The effective rotational Hamiltonian of a molecule rotating in an exterior magnetic field may be written as [1]:

$$\mathcal{H}_{\text{eff}} = \frac{\hbar^2}{2}\mathbf{J}^{\text{t}}\cdot\mathbf{I}^{-1}\cdot\mathbf{J} - \frac{\mu_0}{2}\{\mathbf{J}^{\text{t}}\cdot\mathbf{g}^{\text{t}}\cdot\mathbf{H}+\mathbf{H}^{\text{t}}\cdot\mathbf{g}\cdot\mathbf{J}\} - \tfrac{1}{2}\mathbf{H}\cdot\boldsymbol{\chi}\cdot\mathbf{H} - \frac{1}{c}\mu_{\text{el}}\cdot(\mathbf{V}_0\times\boldsymbol{H})$$

$\mathbf{J}^{\text{t}} = (J_a, J_b, J_c)$
= one row matrix corresponding to the angular momentum operator in units of $\hbar$ and referred to the molecular principle inertia axis system. (Super t denotes the transposed matrix.)

$\mathbf{I}^{-1}$ = matrix corresponding to the inverse of the molecular moment of inertia tensor.

$\mu_0 = \dfrac{|e|\hbar}{2 M_{\text{p}} c}$
= nuclear magneton.

$\mathbf{H}^{\text{t}} = (H_a, H_b, H_c) = (\cos a Z, \cos b Z, \cos c Z)\,H_Z$
one row matrix corresponding to the magnetic field vector $\boldsymbol{H}$ referred to the principle inertia axis system (the exterior field is assumed to point in the direction of the space fixed Z-axis).

$\mathbf{g}$ = Matrix corresponding to the molecular g-tensor. For symmetric top molecules $\mathbf{g}$ and $\mathbf{I}^{-1}$ are simultaneously diagonal. Within the rigid nuclear frame approximation the theoretical expressions for the diagonal elements of the g-tensor are given by [2, 3]:

$$g_{aa} = \frac{M_{\text{p}}}{I_{aa}^{(n)}}\left(1+\frac{2}{I_{aa}^{(n)}}\left(\frac{L_a L_a}{\Delta}\right)\right)\cdot\sum_{\nu}^{\text{nuclei}} Z_\nu(b_\nu^2+c_\nu^2) + \frac{M_{\text{p}}}{I_{aa}^{(n)}}\cdot\frac{2}{m}\left(\frac{L_a L_a}{\Delta}\right)$$

and cyclic permutations,

$I_{aa}^{(n)} = \sum_{\nu}^{\text{nuclei}} m_\nu(b_\nu^2+c_\nu^2)$
= nuclear contribution to the moment of inertia tensor,

m_ν, Z_ν = mass and atomic number of the ν-th nucleus,

$$\left(\frac{L_a L_a}{\Delta}\right) = \sum_n \frac{\langle 0|L_a|n\rangle\langle n|L_a|0\rangle}{E_0-E_n}$$
= perturbation sum running over the excited electronic states,

$$L_a = \frac{\hbar}{i}\sum_{\varepsilon}^{\text{electrons}}\left(b_\varepsilon\frac{\partial}{\partial c_\varepsilon} - c_\varepsilon\frac{\partial}{\partial b_\varepsilon}\right)$$
= a-component of the electronic angular momentum operator,

$\boldsymbol{\chi}$ = matrix corresponding to the molecular susceptibility tensor. Within the rigid nuclear frame approximation its diagonal elements are given by [4, 3]:

$$\chi_{aa} = -\frac{e^2}{4 m c^2}\langle 0|\sum_{\varepsilon}^{\text{electrons}}(b_\varepsilon^2+c_\varepsilon^2)|0\rangle - \frac{e^2}{2 m^2 c^2}\left(\frac{L_a L_a}{\Delta}\right)$$

and cyclic permutations,

μ_{el} = vector of the molecular electric dipole moment,

$\mathbf{V}_0$ = vector of the molecular center of mass velocity.

Different from previous microwave spectroscopical investigations the translational Zeeman effect,

* Part of this work is taken from the thesis of L. Engelbrecht.
Reprint requests to Prof. Dr. D. H. Sutter, Institut für Physikalische Chemie der Universität Kiel, *D-2300 Kiel*, Olshausenstraße 40/60.

Eq. (1, d) which destroys the axial symmetry of $\mathcal{H}_{\text{eff}}$ with respect to rotations about the magnetic field axis has been included explicitly. It accounts for the fact that the Lorentz-forces due to the translational motion, $\boldsymbol{F}_i = (q_i/c)(\boldsymbol{V}_0 \times \boldsymbol{H})$, pulling the positive nuclei ($q_i = Z_i|e|$) in one direction and pushing the negative electrons ($q_i = -|e|$) in the opposite direction, have the same effect as a virtual electric field of size $\boldsymbol{E}_{\text{TL}} = (1/c)(\boldsymbol{V}_0 \times \boldsymbol{H})$. At thermal velocities $\boldsymbol{E}_{\text{TL}}$ is on the order of few V/cm and its contribution may be regarded as a low field Stark effect. As far as the limited resolution of standard microwave spectroscopy is concerned this "translational Stark effect" may be savely neglected for molecules showing a second order Stark effect such as linear and asymmetric to molecules. However in molecules with transitions showing a first order Stark effect such as the $K \neq 0$ transitions of symmetric tops or the E-species lines of molecules with a low barrier methyl top internal rotation it has to be accounted for. It does not merely lead to a symmetric broadening of the absorption lines as was implicitly assumed in all previous investigations. In the following we will demonstrate how the overall appearance of the Zeeman multiplets is changed due to the translational Zeeman contribution and that considerable corrections have to be applied to the published $g_{||}$-values.

The basic principles are illustrated in Figure 1. If the molecule has zero velocity perpendicular to the magnetic field, there is no translational Zeeman effect [case (a) in Figure 1]. The magnetic field determines the axis of quantization with (1, b) and (1, c) causing the angular momentum vector $\hbar \boldsymbol{J}$ to precess about the magnetic field axis. On the other hand, for a molecule at high translational velocity perpendicular to the magnetic field, the torque of the virtual electric field acting on the molecular electric dipole moment dominates. It causes the molecule to precess essentially about the $\boldsymbol{E}_{\text{TL}}$-axis, which now becomes the axis of quantization [case (b) in Figure 1].

We now turn to the selection rules which may be understood already in a classical picture. In an experimental arrangement as shown in the insert of Fig. 2 the electric vector, $\boldsymbol{E}_{\text{MW}}(t)$, of the incident microwave radiation, which in the TE_{10}-mode of propagation is polarized perpendicular to the broad face of the waveguide absorption cell, is parallel to the magnetic field serving as the quantization axis at low perpendicular velocities. Thus the rapidly oscillating torque due to $\boldsymbol{E}_{\text{MW}}(t)$:

$$\hbar\, d\boldsymbol{J}/dt = \boldsymbol{\mu}_{\text{el}} \times \boldsymbol{E}_{\text{MW}}(t)$$

which at resonance causes the rotational transition, is perpendicular to the quantization axis. This results in the "low velocity selection rule" $\Delta M = 0$,

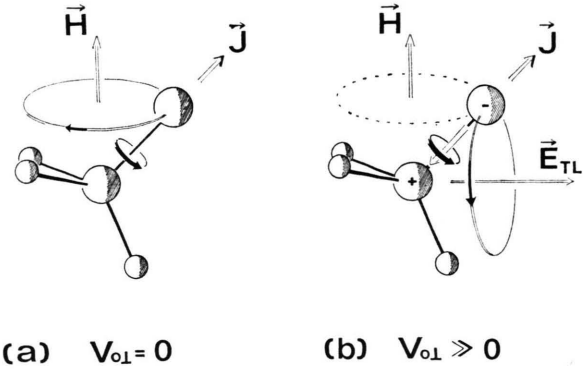

Fig. 1. The magnetic effects on the molecular rotation of the CH_3F molecule rotating about its symmetry axis are shown for two limiting cases.

a) The molecule has zero translational velocity. The small rotational magnetic moment causes a precession about the magnetic field axis (rotational Zeeman effect).

b) The molecule has a high translational velocity perpendicular to the magnetic field (pointing towards the reader). The corresponding translational Stark field $\boldsymbol{E}_{\text{TL}} = (1/c) \cdot \boldsymbol{V}_0 \times \boldsymbol{H}$ exerts a torque on the permanent electric dipole moment which vastly exeeds the torque due to the rotational Zeeman effect and essentially causes to precess about the $\boldsymbol{E}_{\text{TL}}$-axis.

(no change of the angular momentum component in direction of the axis of quantization). With increasing velocity perpendicular to the field the translational Zeeman effect [Eq. (1, d)] becomes more and more important. It not only causes a continuous change in the splittings of the $2J+1$ different sublevels of each rotational state, but also completely changes the selection rules. Since at high field vector is now perpendicular to the new quantition changes from $\boldsymbol{H}$ to $\boldsymbol{E}_{\text{TL}}$, the microwave electric field vector is now perpendicular to the new quantization axis and the selection rules change to $\Delta M = \pm 1$. (Although M looses its meaning as the quantum number for the Z-component of the angular momentum we still keep it for labeling the levels). The change in selection rules is also illustrated in Fig. 2, where for molecules moving at different velocities perpendicular to the exterior field calculated Zeeman patterns are shown for the $J = 1$ to

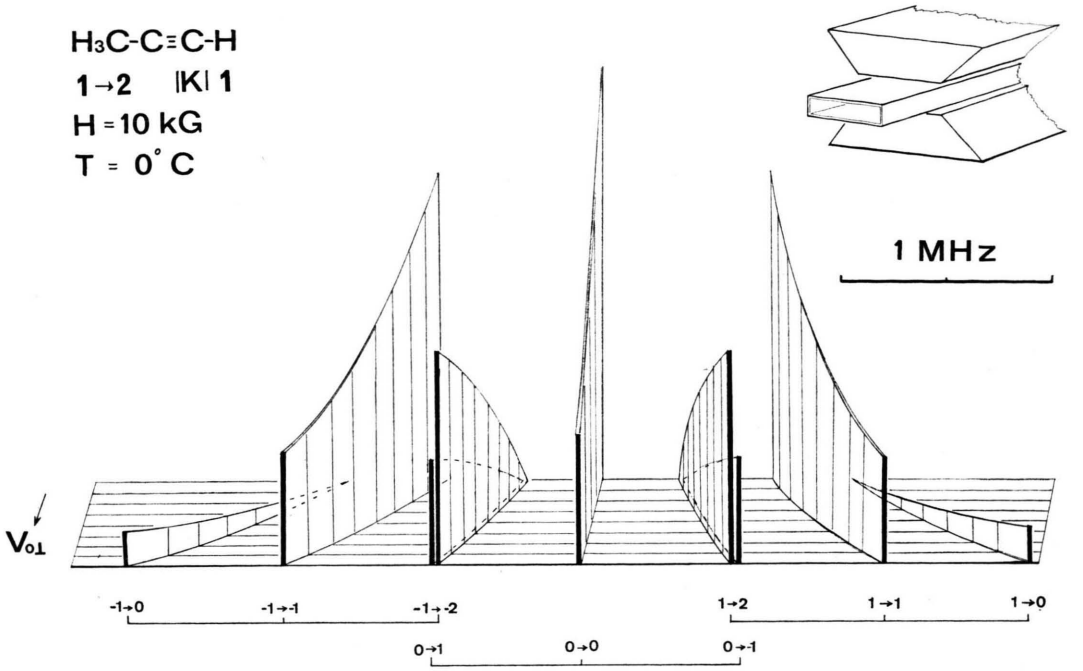

Fig. 2. Calculated Zeeman patterns of the $J=1 \rightarrow J=2$ ($|K|=1$) rotational transition of Methylacetylene. For molecules with increasing perpendicular velocity $V_{0\perp}$ the translational Stark effect becomes more and more important. The transition frequencies are shifted and new transitions appear with increasing intensity. At very high perpendicular velocities the M-selection rule effectively changes from $\Delta M=0$ ($V_{0\perp}=0$) to $\Delta M=\pm 1$ ($V_{0\perp} \gg 0$). The shown patterns cover the velocity range from $V_{0\perp}=0$ to $V_{0\perp}=800$ m/sec.

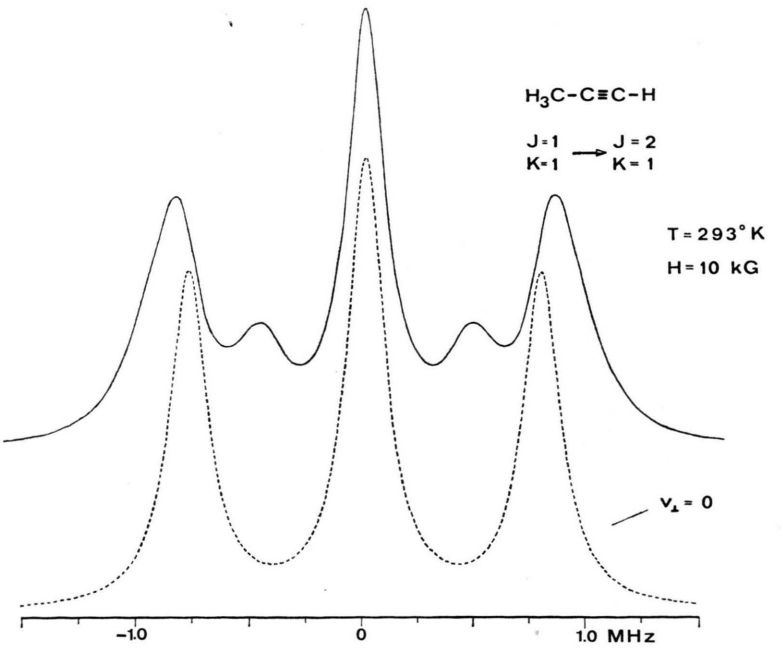

Fig. 3. Calculated line profile for the $J=1 \rightarrow J=2$ ($|K|=1$) rotational transition of Methylacetylene. It results from a superposition of individual spectra such as shown in Fig. 2, each weighted with the appropriate Maxwell-Boltzmann probability. For comparison the dotted line shows the absorption spectrum calculated under the neglect of the translational Stark effect.

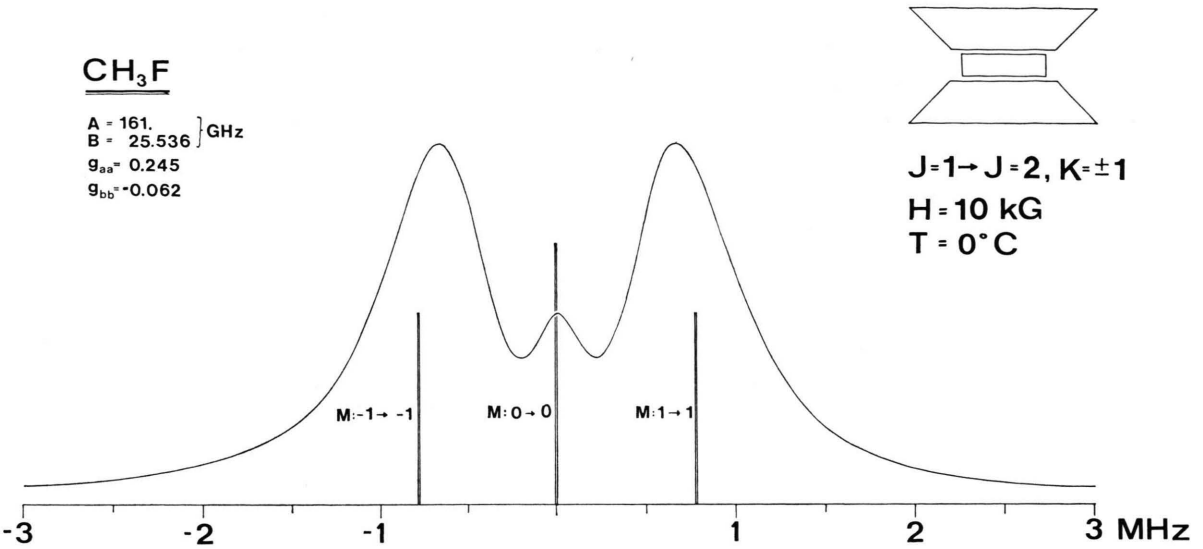

Fig. 4. Calculated line profile for the $J=1\rightarrow J=2$ ($|K|=1$) rotational transition of CH_3F. It closely agrees with the observed spectrum published by Gordy and Cox (Ref. 5). The bars indicate the positions and relative intensities of the Zeeman satellites calculated under neglect of the translational Stark effect. Due to the bigger dipole moment the mixing of the different M-substrates occurs already at rather low perpendicular velocities. This is clearly visible in the line profile from the low intensity remaining at the position of the $M=0\rightarrow M=0$ transition.

$J=2$ ($|K|=1$) rotational transition of methylacetylene. Details of the calculation are given in the Appendix. The observable pattern is obtained weighting each pattern with the appropriate Maxwell-Boltzmann probability:

$$p_{(V_{0\perp})}\,\mathrm{d}V_{0\perp} = (M V_{0\perp})/(kT)\exp\{-M V_{0\perp}^2/2kT\}\,\mathrm{d}V_{0\perp}$$

and summing over the different velocities $V_{0\perp}$ ($V_{0\perp}=|\mathbf{V}_{0\perp}|$).

The result is shown in Fig. 3 (for comparison the dotted curve shows the spectrum calculated under the neglect of the translational Zeeman effect). Under the influence of $\boldsymbol{E}_{\mathrm{TL}}$ the outer satellites have moved further out with the Boltzmann tail clearly visible in the wings and additional peaks due to the new transitions appear in between the original $M=\overset{+}{(-)}1\rightarrow M'=\overset{+}{(-)}1$ and $M=0\rightarrow M'=0$ satellites. In molecules with bigger dipole moments the change in selection rules occurs already at lower

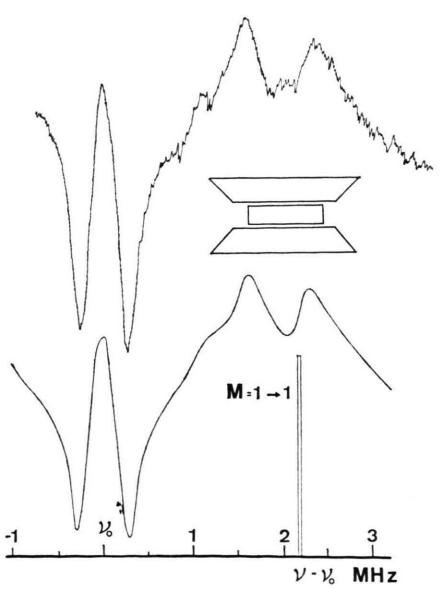

Fig. 5. Part of the Zeeman pattern of a rotational transition of CH_3BF_2 recorded with a microwave spectrometer using 33 kHz Stark effect modulation. The magnetic field strength was 24085 Gauss. The observed lineprofile actually consists of a superposition of two spectra, one with the modulation field off (pure Zeeman spectrum) which is written upwards and one with the modulation field on (Stark-Zeeman spectrum) which is written downwards. The negative lobes close to the zero field frequency ν_0 originate from the $M=0$ substates. The lower trace shows the corresponding lineprofile calculated under inclusion of the translational Stark effect. For molecules with zero translational velocity perpendicular to the magnetic field the spectrum would consist of single line at the position of the vertical bar. The corresponding Stark lobe is mooved out far to the right. At zero perpendicular velocites the $M=0$ substate are essentially unmodulated at Stark fields close to 22 V/cm as were used for this recording.

velocities with correspondingly heigher Boltzmann weight factors thus causing even greater changes with respect to the line pattern expected under the neglect of (1, d). As an example Fig. 4 shows a calculated line pattern for the $J=1$ to $J=2$ ($|K|=2$) transition of Methylfluoride, which is in close agreement with the experimentally observed pattern [5]. Figure 5 shows the importance of the translational Stark effect contribution in an E-species transition of CH_3BF_2.

In order to give an idea of the order of magnitude of the errors introduced into the analysis of the Zeeman data through the neglect of (1.d), we have recalculated $g_{||}=g_{aa}$ for Methylacetylene and Methylfluoride from published line profiles [5–7] giving $g_{aa}=+0.245$ (CH_3F) and $g_{aa}=+0.295$ (CH_3CCH) as compared to the originally published values calculated under the neglect of (1,d): $g_{aa}=0.265\pm0.008$ (CH_3F) [6] and $g_{aa}=+0.312\pm0.002$ (CH_3CCH) [7]. The corrected values should be considered only as preliminary since the cell temperature had to be assumed in the evaluation of the line profiles. However the discrepancy of the values calculated with and without inclusion of (1,d) leads to the conclusion that all $g_{||}$-values of symmetric tops determined from microwave rotational Zeeman effect studies should be reexamined. The molecular electric quadrupole moments calculated from the published g-values are certainly incorrect far outside the quoted uncertainties.

Appendix

For a symmetric top molecule with the a-axis, the axis of least moment of inertia, parallel to the symmetry axis, as is the case for instance in CH_3F and CH_3CCH, the effective Hamiltonian given in Eq. (1) reduces to:

$$\mathcal{H}_{\text{eff}}=\frac{\hbar^2}{2I_{aa}}J_a^2+\frac{\hbar^2}{2I_{bb}}(\mathbf{J}^2-J_a^2) \tag{A.1 a}$$

$$-\mu_0 H_Z\{g_{aa}\cos a\,Z\,J_a+g_{bb}[\cos b\,Z\,J_b+\cos c\,Z\,J_c]\} \tag{A.1 b}$$

$$-\tfrac{1}{2}H_Z^2\{\chi_{aa}\cos^2 a\,Z+\chi_{bb}(1-\cos^2 a\,Z)\} \tag{A.1 c}$$

$$-\mu_{\text{el}_a}\cdot|\boldsymbol{E}_{\text{TL}}|\cos a\,Y\,. \tag{A.1 d}$$

In (1,d) the space fixed Y-axis is choosen to point in the direction of the virtual electric field of $\boldsymbol{E}_{\text{TL}}$ in order to avoid complex matrix elements in the numerical calculation. This is an individual choise for each molecule, but of cause it has no effect on the energy levels, transition frequencies and intensities.

For the further treatment the Hamiltonian matrix corresponding to Eq. (A,1) is most conveniently set up within the eigenfunction basis of the symmetric top [Eq. (A,1,a)]. With the rotational energies on the order of several GHz, the field dependent matrixelements which are only on the order of few MHz may be treated as a perturbation and within the resolution of microwave spectroscopy all matrix elements connecting different rotational states J, K may be neglected. The remaining nonvanishing matrixelements are given by:

$$\begin{aligned}\langle J,K,M|\mathcal{H}_{\text{eff}}|J,K,M\rangle=&\frac{\hbar^2}{2I_{aa}}K^2+\frac{\hbar^2}{2I_{bb}}\\&\cdot\{J(J+1)-K^2\}\\&-\mu_0 H_Z M\left\{g_{aa}-(g_{bb}-g_{aa})\frac{K^2}{J(J+1)}\right\}\\&-\frac{H_Z^2}{3}\frac{3M^2-J(J+1)}{(2J-1)(2J+3)}\left[1-\frac{3K^2}{J(J+1)}\right]\\&\cdot(\chi_{bb}-\chi_{aa})\end{aligned} \tag{A.2}$$

from (A,1,a) through (A,1,c) and

$$\begin{aligned}&\langle J,K,M|\mathcal{H}_{\text{eff}}|J,K,M\pm1\rangle\\&\quad=-\mu_{\text{el}_a}\cdot|\boldsymbol{E}_{\text{TL}}|\frac{K\sqrt{J(J+1)-M(M\pm1)}}{2J(J+1)}\end{aligned} \tag{A.3}$$

from (A,1,d).

The isotropic contribution $\frac{1}{3}(\chi_{aa}+\chi_{bb}+\chi_{cc})H_z^2$, which drops out of the energy differences in rotational transitions, has been neglected already in Equation (A,2). In Fig. A.1 numerical values are given for the $2J+1$ by $2J+1$ M submatrix of the $J=2$, $|K|=1$ rotational state of a methylfluoride molecule moving at a speed of 267 m/sec perpendicular to the exterior magnetic field. This velocity corresponds to the maximum of the Maxwell-Boltzmann probability distribution at a temperature $T=293$ °K. Similarly all other rotational states J', K' lead to square submatrices of rank $2J'+1$ with off diagonal elements due to the translational Zeeman effect (A,1,d).

In order to calculate the Zeeman patterns shown in Fig. 2 the M-submatrices of the two rotational states involved in the transition were numerically diagonalized by the Jacobi procedure and the transition cosine matrix elements, initially set up within the symmetric top basis, were subjected to the cor-

M \ M'	-2	-1	0	1	2
-2	-0.165 - 0.01	-0.415	0	0	0
-1	-0.415	-0.083 +0.005	-0.508	0	0
0	0	-0.508	0 +0.01	-0.508	0
1	0	0	-0.508	0.083 + 0.005	-0.415
2	0	0	0	-0.415	0.165 - 0.01

Fig. A.1. The $2J+1$ by $2J+1$ M-submatrix (A.2, A.3) of the $J=2$, $|K|=1$ rotational state of a methylfluoride molecule is shown for the $V_{0\perp}$-value of 267 m/sec corresponding to the maximum of the Maxwell-Boltzmann probability distribution at a temperature of 293 °K. The M-independent rotational energies of A.2 are dropped from the matrix. Following values are used: $H_Z=10$ kG, $g_{aa}=+0.245$, $g_{bb}=-0.062$, $\chi_{bb}-\chi_{cc}=8.5\cdot10^{-6}$ erg/G²Mol, $\mu_{el_a}=1.847$ Debye. The diagonal matrix elements are divided in the g-part (first term) and the susceptibility part (second term).

responding unitary transformation. At intermediate velocities transitions are possible between all M-sublevels of the lower and upper rotational state with intensities strongly depending on the g- and χ-values on the electric dipole moment, and on the magnitude of the virtual electric field. In Methylacetylene only the transitions corresponding to "$\Delta M=0$" and "$\Delta M=\pm1$" turn out to have appreciable intensities. On the other hand in Methylfluoride the individual patterns are rather complicated with intensities oscillating between different transitions in dependence on the increasing translational velocity. Of cause at the limit to high translational speeds the pattern approaches a pure $\Delta M=\pm1$ spectrum as expected from the classical picture discussed above.

As long as no additional fields (for instance an electric Stark-field) need to be considered, the Zeeman patterns for $+K$ and $-K$ are identical although with different assignments of the transitions. In the presence of an exterior Stark-field in the Z-direction the K degeneracy is removed and the above described procedure has to be carried out for both K-values under inclusion of the corresponding potential energy term $-\mu_{el_a}\cdot E_Z\cdot\cos a\,Z$. The observed pattern is then obtained as a superposition of the $+K$ and $-K$ multiplets for the different velocities.

Acknowledgement

The calculations were done on the PDP 10 computer of the "Rechenzentrum der Universität Kiel". The financial support of the "Deutsche Forschungsgemeinschaft" and the "Fonds der Chemie" are gratefully acknowledged.

[1] D. Sutter, A. Guarnieri, and H. Dreizler, Z. Naturforsch. **25a**, 222 [1970]; D. Sutter, A. Guarnieri, and H. Dreizler, Z. Naturforsch. **25a**, 2005 [1970].
[2] J. R. Eschbach and H. W. P. Strandberg, Phys. Rev. **85**, 24 [1952].
[3] D. Sutter, Z. Naturforsch. **26a**, 1644 [1971].
[4] J. H. Van Vleck, The Theory of Electric and Magnetic Susceptibilities, Oxford University Press, Chap. X, 1932.
[5] J. T. Cox and W. Gordy, Phys. Rev. **10**, 1298 [1956].
[6] C. L. Norris, E. F. Pearson, and W. H. Flygare, J. Chem. Phys. **60**, 1758 [1974].
[7] R. L. Shoemaker and W. H. Flygare, J. Amer. Soc. **91**, 5417 [1969].